Doppler Radar Analysis on the Characteristics of Eyewall and Rainbands Associated with Supertyphoon Bilis (2000) by the Influence of Taiwan Orography

Chih-Hsien Wei (魏志憲)
Department of Military Meteorology, Air Force Institute of Technology
email：g950101@gmail.com

Tai-Hwa Hor (何台華)
General Education Center, Lunghwa University of Science and Technology
email：thhor@mail.lhu.edu.tw

Jian-Liang Wang (汪建良)
Department of Environmental Information and Engineering, National Defense University
email：moredose.w@gmail.com

Abstract

This paper focuses on the examination of rainband variations associated with Typhoon Bilis (2000), vertical structures and radial wind fields while the system was under the influence of Taiwan high topography before landfall.

Typhoon Bilis possessed the feature of well organized double eyewall with an approximate circular shape and a period of nearly 2 hours in counterclockwise rotation, and its inner and outer rainbands were distinctive while the storm center was about 100 km away from the radar site. Convective cells inside the rainbands featured outward propagation at the first quadrant, and inward migration to outer eyewalls at the second and third quadrants. The former one became a linear rainband and developed well organized with propagating speed twice larger than that in typhoon entity. The later one triggered the development of outer eyewalls.

Basically, the low level confluence was the critical mechanism to enhance the intensity of wind speed at the second quadrant in the lower layer (below 1.0 km in altitude), appearing the reverse distribution of peak Doppler wind at the right and left quadrants. However, this phenomenon became more obscure while the storm was getting closer to the Taiwan terrain due to the severity in intensity and the well organization of the entity which was quite different from the slight typhoon case (Hor et al. 2005). A conceptual model for the super typhoon case under the great influence of Taiwan terrain was constructed, showing the non-tilting appearance in the vertical and the normal distribution of peak winds in the entire layer.

Key words: Double eyewall, Outer rainbands, Confluence

1. Introduction

The lack of meteorological data over the vast Pacific Ocean and the strong interaction between typhoon circulation and CMR are two major factors that make the forecasting of typhoons in the vicinity of Taiwan highly challenging. The numerical models become a crucial research vehicle to improve the knowledge. However, increasing observations are needed for model initiation and verification (Wu and Kuo 1999). By using the observational data collected by the Green Island Doppler weather radar (hereafter, GRI), the study focus on the mesoscale analysis of typhoon Bilis, which is categorized as severe typhoon with northwestward moving path, before and under the Influence of Taiwan Terrain. The study is comparable with typhoon Otto (1998) (Hor et al. 2005), which is the first typhoon captured by GRI radar.

Based on the warning report announced by the Joint Typhoon Warning Center (JTWC) (Fig. 1), Typhoon Bilis built up on the ocean out of eastern Philippines at 0600 UTC 19 August 2000 (Fig. 1). It moved northwestward steadily in speed of 15 km/h. The typhoon was committed to be super typhoon (maximum wind speed > 64 ms^{-1}) from 1200 UTC 21 to 1500 UTC 22 August 2000. During the period, it made landfall on the southeastern coast of Taiwan by 1430 UTC 22 August. The affected duration of storm over the island was almost 3.5 hours. It was remarkable that the propagation path for both typhoon Bilis and Otto (1998) are comparable while they were in the vicinity of Green Island before landfall. Even their announced intensity are considerately different, such data collection from Doppler radar observation for the north-northwestward moving typhoon is rarely to find. This is viable for the study to investigate the influence of Taiwan topography for the slight and severe typhoons, based on the hypothesis of the same moving path.

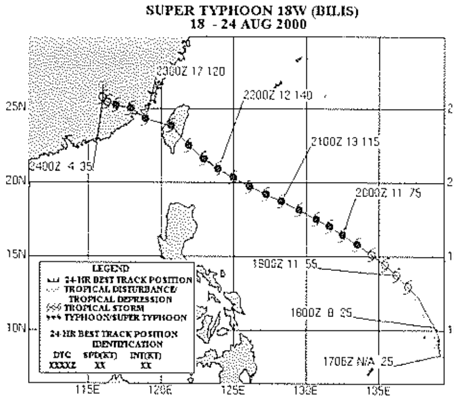

Fig. 1 Track map of Typhoon Bilis (2000) reported by the Joint Typhoon Warning Center (JTWC).

2. Mesoscale behaviors of Typhoon Otto under the Influence of Taiwan Orography

As the typhoon was approaching the sea shore closely since 1100 UTC 22 August 2000 (Fig. 3), the pattern of its double eyewall could be determined clearly. Its organization was getting distinctive at the second and third quadrant during this period with a quasi axial-symmetric feature. Accordingly, the rotation of eyewall was easy to identify, which has a period of approximate 2 hours. And it is appropriate to learn that the diameter of the quasi-circular inner eyewall was around 35 km based upon the analysis of the Doppler mode pictures. In addition, some convective cells distributed over the first and second quadrants could be distinguished from the eyewall. These convective cells concentrated at the outer region of the first quadrant were propagating northwestward, and had an angular difference larger than 10 degrees with respect to the moving direction of typhoon (~325 deg). Their mean propagating speed was 70-80 km hr^{-1} relative to the ground (~35 km hr^{-1} relative to the storm motion), about two times larger than that of the typhoon (35-40 km hr^{-1}). They became a linear rainband parallel to the coastal mountains in the northnortheast-southsouthwest orientation before landfall. The rainband was intensified just off the sea shore and still kept its strength even encounter the terrain.

The vertical structures of rainbands from 1045 UTC to 1145 UTC on the third quadrant of the typhoon (along the 225 or 230 degree in azimuth, Fig. 4) shows that the strength of echoes for the inner eyewall, outer eyewall and outer rainband were similar unexpectedly. The height of the area enclosed by 20 dBZ for these rainbands was also almost alike, except the eyewall strengthened and extended to 10 km in height afterward. The radii of the eye and eyewall were 20 km and 50 km steadily, indicating that the eyewall replacement never occurred during the period. However, the outer rainband propagated inward and merged into the eyewall, which seemed to play a significant role to maintain the development of the eyewall. It also indicated the structure of typhoon was more organized at the second and third quadrants, which is corresponding to the study of typhoon Otto. The eyewall and outer rainband extends vertically with outward slantwise of around 70 degree. And the vertical distribution of accompanying maximum Doppler velocity tilted with the similar inclination. Nevertheless, the vertical axis of maximum wind associated with inner eyewall leaned outward by 70 degree, where the axis of echoes extended steeply.

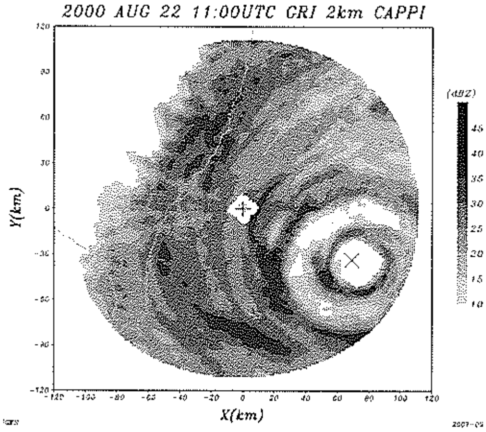

Fig. 2 The constant altitude plan positive indicator (CAPPI) of reflectivity (dBZ) in the altitude of 2 km at 1100 UTC on 22 August 2000. The radar site is located at [0,0]. Symbol "x" stands for typhoon center.

3. The circulation variations of the storm entity by the orographical effect

The temporal variation for such a feature between 1015 UTC and 1145 UTC 22 August is described in Table 1 elaborately. The left quadrant in the lower portion (below 1 km in altitude) from 1015 UTC to 1115 UTC owned stronger Doppler velocity than that in the right quadrant, and the upper portion had the opposite feature. However, both maximum winds were nearly the same while getting closer to the terrain in 1130 UTC (~67 km away from the radar) and 1145 UTC (~59 km away from the radar). The reverse distribution of maximum winds in the slight Typhoon Otto (1998) case was also observed. It existed at 1 km level while the typhoon center was located at 109 km away from the radar site, and gradually extended to 2 km level at the last volume scan. The difference between positive and negative peak wind speeds was prominent for levels below 1.5 km, and was confined to be 1 m/s difference in magnitude at the 1.5 km level, revealing that the reverse situation of maximum wind is critical at the lower level. In the Otto case, however, the reverse mode of Doppler wind in the lower portion became more pronounced while getting closer to the mountain. The confluence of the southwesterly flow triggered by the farther outer circulation of the typhoon around the island and the northwesterly flow from the inner circulation of the typhoon also played role to accelerate the air speed at the second quadrant of the system at lower levels. However, the orographic blocking effect did not significantly influence on the circulation at upper levels. The typhoon kept its primary feature with the stronger wind field at the right quadrant and the weaker one in the left quadrant. The present study for super Typhoon Bilis verifies the orographic blocking on the maximum wind of inner circulation in the first quadrant at lower levels again. However, such an effect only affects the flow of typhoon at the level below 1 km, and it is hard to be examined as Bilis closes to the coast, probably relating to its severity in intensity and the well organization of the system.

4. Discussion and Summary

After 0945 UTC of 22 August, the typhoon Bilis kept approaching the southeast coast of Taiwan and its structure in Doppler velocity field was expected to have distinctive changes in the vertical. At lower levels (less than 1.0 km in altitude) at 1100 UTC on 22 August (Fig. 5), the Doppler velocity fields showed that the maximum wind speeds at the second quadrant were more intense than those at the first quadrant. However, the Doppler velocity fields at the upper levels had the opposite situation. The findings based on the study of slight Typhoon Otto illustrate that the maximum wind at the second quadrant appears larger peak radial wind at lower level due to the low level confluence between the southwesterly flow triggered by the farther outer circulation of the storm around the Taiwan island and the northwesterly flow near the inner circulation of storm itself. The similar situation occurs in the Bilis case. Basically, the low level confluence is still the critical mechanism to enhance the intensity of wind speed at the second quadrant in the lower layer (below 1.0 km in altitude). However, the phenomenon becomes more obscure while the storm is getting closer to the Taiwan terrain due to the severity of Typhoon Bilis. Based upon the above findings, a conceptual model for the super typhoon case under the influence of Taiwan terrain can be integrated and constructed, which doesn't possess the tilting appearance in the vertical as well as the reverse distribution of peak positive and negative winds in the lower layer, comparing with the slight typhoon case (Otto, 1998).

References

王時鼎、謝信良、鄭明典、葉天降，1998：侵台颱風流型與颱風路徑走向間之關係研究，中央氣象局天氣分析與預報研討會論文彙編，台北市，268-275。

Black, M. L. and Willoughby, H. E., 1992: The Concentric Eyewall Cycle of Hurricane Gilbert. *Mon. Wea. Rev.*,120, 945-947.

Hor, T.-H., Wei, C.-H., and Chang, M.-H., 2005: Doppler Radar Analysis of Typhoon Otto (1998) - Characteristics of Eyewall and Rainbands with and without the Influence of Taiwan Orography. *J. Meteor. Soc. Japan*, 83, 1001-1023.

Kuo, H.-C., and Williams, R. T., and Chen, J.-H., 1999: A Possible Mechanism for the Eye Rotation of Typhoon Herb. *J. Atmos. Sci.*, 56, 1659–1673.

Marks, F. Jr. and Houze, R. A. Jr., 1987: Inner Core Structure of Hurricane Alicia from Airborne Doppler Radar Observations. *J. Atmos: Sci.*, 44, 1296-1317.

Willoughby, H. E., Marks, F. D., and Feinberg, R. J., 1984: Stationary and Moving Convective Bands in Hurricanes. *J. Atmos. Sci.*, 41, 3189-3211

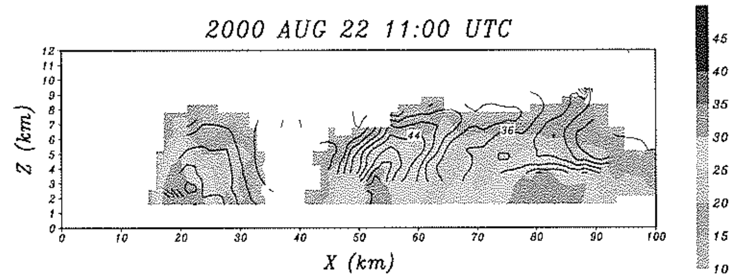

Fig. 3 The vertical cross section of reflectivity (dBZ) and Doppler wind (m/s) across Typhoon Bilis (2000) based upon the Doppler weather radar data collected by the Green Island radar station. The position at X = 0 km stands for the typhoon center, and the positive x-axis points to the southwest direction (225 deg).

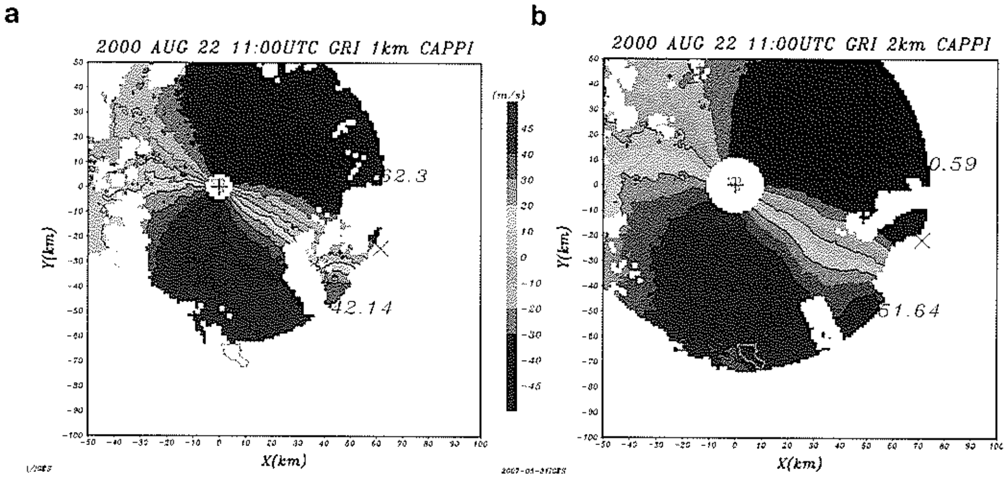

Fig. 4 The CAPPIs of Doppler velocity at (a) 1 km and (b) 2 km level at 1100 UTC 22 August 2000. The radar site is located at [0,0]. Symbol "x" stands for typhoon center.

Table 1. The peak positive and negative Doppler velocities measured by the Green Island weather radar inside Typhoon Bilis from 1015 UTC 1145 UTC 22 August 2000. The shaded area represents the reverse phenomena of Doppler peak winds in the lower portion of typhoon.

Time Level	1015 UTC	1030 UTC	1045 UTC	1100 UTC	1115 UTC	1130 UTC	1145 UTC
1.0 km	-40.7	-36.3	-59.0	-56.4	-59.8	-65.2	-64.9
	+54. 3	+56.4	+58.2	+64.5	+62.8	+60.9	+63.5
1.5 km	-65.7	-65.2	-65.2	-63.8	-59.8	-65.2	-64.4
	+58.6	+63.5	+57.7	+57.5	+52.4	+60.2	+59.6
2.0 km	-66.7	-65.6	-65.2	-63.5	-66.1	-65.2	-63.9
	+57.9	+55.3	+60.0	+57.5	+54.3	+55.7	+56.8
2.5 km	-64.6	-65.4	-65.2	-63.0	-63.7	-65.2	-64.3
	+56.3	+55.3	+53.9	+52.7	+53.9	+58.0	+54.1
3.0 km	-63.7	-64.8	-65.2	-62.7	-67.2	-65.2	-65.7
	+54.9	+54.2	+53.1	+52.0	+53.0	+56.5	+54.0
4.0 km	-63.8	-63.7	-64.8	-63.7	-67.7	-65.2	-65.7
	+53.1	+55.3	+49.7	+50.0	+51.9	+62.8	+52.9
Distance between typhoon center and radar	98 km	92 km	89 km	77 km	74 km	67 km	59 km